CFD Report of a Subsonic Study of the NASA N2A Hybrid Wing-Body Using StarCCM+

FH Aachen – University of Applied Sciences
Department of Aerospace Engineering

A k-ω SST turbulence model in combination with a Polyhedral Mesher approach is used to calculate the effects of subsonic flow (Mach No.=0.2) on the NASA Hybrid Wing Body (HWB) aircraft in a simplified N2A configuration (without considering engine nacelles and its effects on the flow simulation). The flow behavior around the body is examined in a cruise configuration, with special focus at the leading edge, trailing edge and the vertical stabilizer. Besides the lift and drag coefficients, the pressure coefficient distribution at different positions of the half span is calculated for various angles of attacks. These results are then compared to experimental wind tunnel data and various study reports. The computed results are in agreement with the experimental data as well as with simulations carried out by other research facilities. However, minor deviations are observed in the magnitude of the lift and drag coefficient as well as major differences in the pressure coefficient distribution over the chord length.

Authors:	Lucas Schurbaum, Yash Vijaykumar Gandhi, Shreyas Ashwin Sunder
Advisors:	Prof. Dr. M. Havermann, Prof. Dr. F. Janser, F. Götten
Group No.:	6
Submission date:	25.01.2020

Table of Contents

List of Figures

List of Tables

Symbols

Re	Reynolds number	$[-]$
Ma_∞	Mach number	$[-]$
q_∞	Dynamic pressure	[Pa]
c_ref	Reference chord	[m]
S_ref	Reference area	$[m^2]$
T_∞	Temperature	[K]
μ_∞	Dynamic viscosity	[Pa s]
ρ_∞	Density	$\left[\frac{kg}{m^3}\right]$
P_∞	Reference pressure	[Pa]
u_∞	Freestream velocity	$\left[\frac{m}{s}\right]$

1. Introduction

A low-speed experimental investigation was conducted on a 5.8% scale Hybrid Wing Body configuration in the NASA Langley 14- by 22-Foot Subsonic Tunnel. This Hybrid Wing Body (HWB) configuration incorporates twin, podded nacelles mounted on the vehicle upper surface between twin vertical tails. This HWB configuration was developed to meet the reduced noise and reduced fuel burn goals as well as to assess its low-speed aerodynamic characteristics. The wind tunnel experiments covered several geometric variations, including wing-body alone (no nacelles or stabilizing fins), a leading-edge droop (slat) for improving high lift performance and the deflection of rear controls.

The aim of this study is to achieve the results that have been obtained by the test facility via CFD simulation in StarCCM+ for the N2A model in cruise configuration. A k-ω SST turbulence model combined with a polyhedral mesh is used to compute the lift and drag coefficients for three different AoAs. In addition, the pressure coefficient distribution at different locations on the half span as well as on the whole body's surface area are visualized. The simulated data shall then be compared with the available experimental data.

2. Geometry

The photo below depicts the HWB in cruise configuration i.e., the wing leading edges are not drooped but blended with the wing. To decrease the computational effort only one half of the plane-symmetric body was used for the simulation. In contrast to the wind tunnel model, the engines and nacelles of the N2A aircraft were not modelled in this simulation for the sake of simplicity. A bullet shaped flow field, 20 model lengths in diameter and 25 for the overall length, was used to project the free stream of the wind tunnel and is shown below:

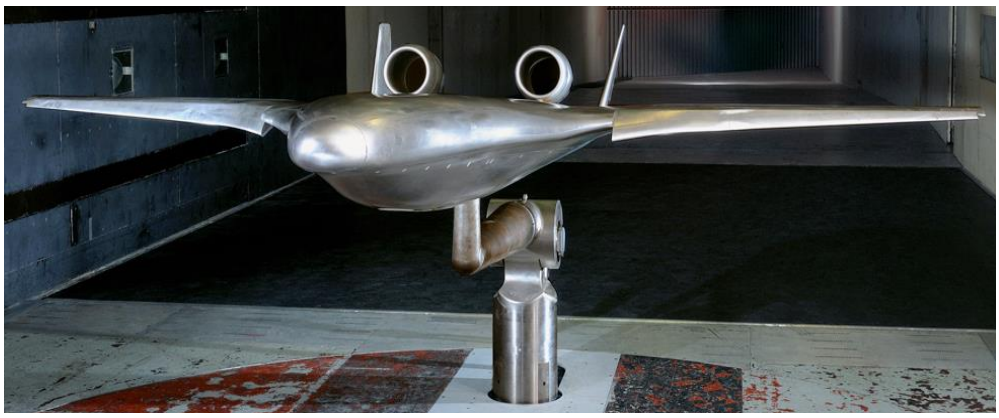

FIGURE 1 5.8% SCALED N2A WIND TUNNEL MODEL WITH DROOPED LEADING EDGE

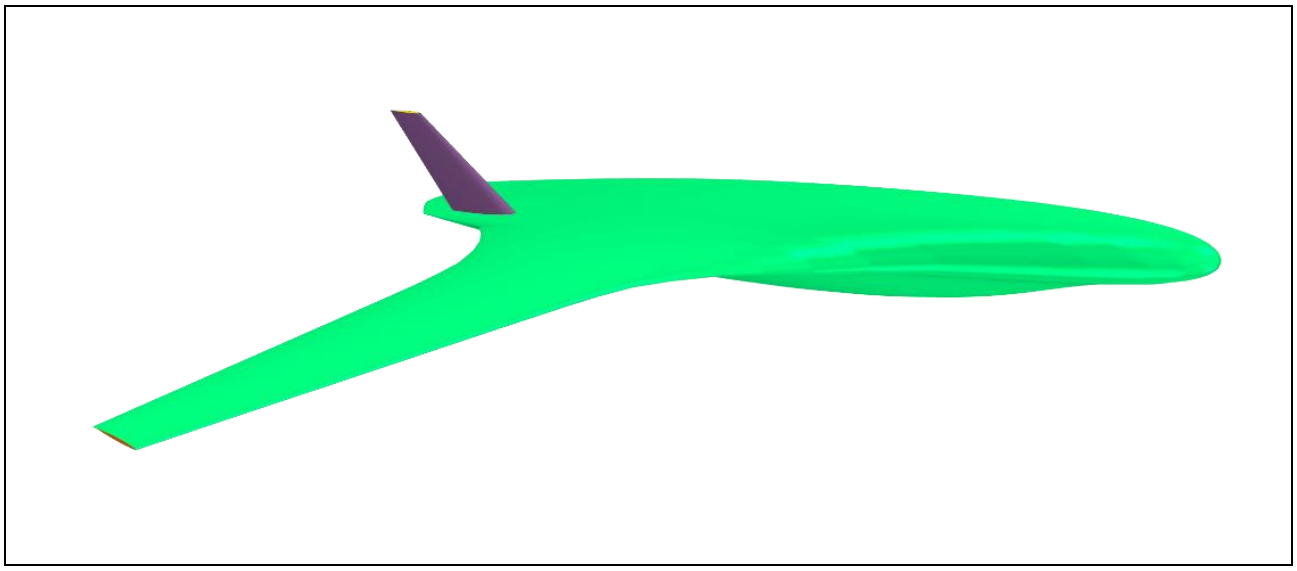

FIGURE 2 ISOMETRIC VIEW OF THE USED SIMULATION MODEL IN STAR CCM+

3. Model Description

3.1 Boundary Conditions

For the CFD simulation, the following parameters (similar to the wind tunnel testing conditions) are used:

Test Parameter	Value
Re	6.6*10^6
M_∞	0.2
q_∞	2872.8 Pa
c_ref	1.54 m
S_ref	3.112 m^2 (Full model)
Fluid	Air

TABLE 1 INITIAL PARAMETERS FOR THE CFD SIMULATION (TAKEN FROM THE WIND TUNNEL DATA)

Using Sutherland's law for the dependency between dynamic viscosity and temperature the remaining boundary conditions can be calculated:

Calculated Parameter	Value
T_∞	300 K
μ_∞	1.846*10^-5 Pa s
ρ_∞	1.1391 kg m^{-3}
p_∞	98.1156 kPa
u_∞	69.45 m s^{-1}

TABLE 2 CALCULATED (PHYSICAL) PARAMETERS FOR THE CFD SIMULATION

The resulting velocity magnitude measures 69.45 ms^{-1} and is applied in the AoA coordinate frame at the inlet of the flow field. The outlet is modelled with no offset to the calculated reference pressure.

3.2 Physical Setup

The combination of a k-ω turbulence model with shear stress transport (SST) formulations offers good behavior at near wall regions as well as in the free stream and avoids extremely high sensitivity to the inlet free-stream turbulence properties. However, it is important to mention that this model tends to produce extremely high turbulence levels at stagnation regions and at regions with strong accelerations. A segregated flow solver was used due to the low velocity air flow.

A steady state solver was used for all AoA but was changed to a coupled flow solver at an AoA 12.53^0 to check the effect of turbulence on the solver. It was observed that the coupled solver made little to no difference to the solution obtained. A segregated flow solver was used as the Mach number of the flow in the flowfield was small and segregated flow solvers work better for low-speed flows where shock waves are not expected. Additionally, solution interpolation and cell quality remediation models were used to get smoother and more stable graphs.

3.3 Mesh

For the validation of the NASA N2A CFD model a polyhedral, automated mesh was used. A prism layer mesh (20 layers) was used to model the boundary layer in the vicinity of the N2A model. Mesh refinements were created at regions where interactions between the flow and the N2A model were expected and where the automated mesh could not resolve the flow-body interactions sufficiently. The regions for the mesh refinements are the main wing, the trailing edges of the body, tip of the wing and the tip of the vertical stabilizer. Furthermore, the thickness of the boundary layer was given for 4 areas: the main fuselage (reference length = c_ref), the vertical stabilizer (reference length = 0.15m), the nose of the fuselage (reference length = 0.021m) and the half wingspan. The boundary layer was later disabled at the nose as the near core aspect ratio was 2.0. The wingspan had two control volumes (inner and outer) as shown in Fig 3 to fix the bad cell quality at the intersection of the fuselage and the wing as well as increase number of cells at the outer part of the wing for a more accurate result.

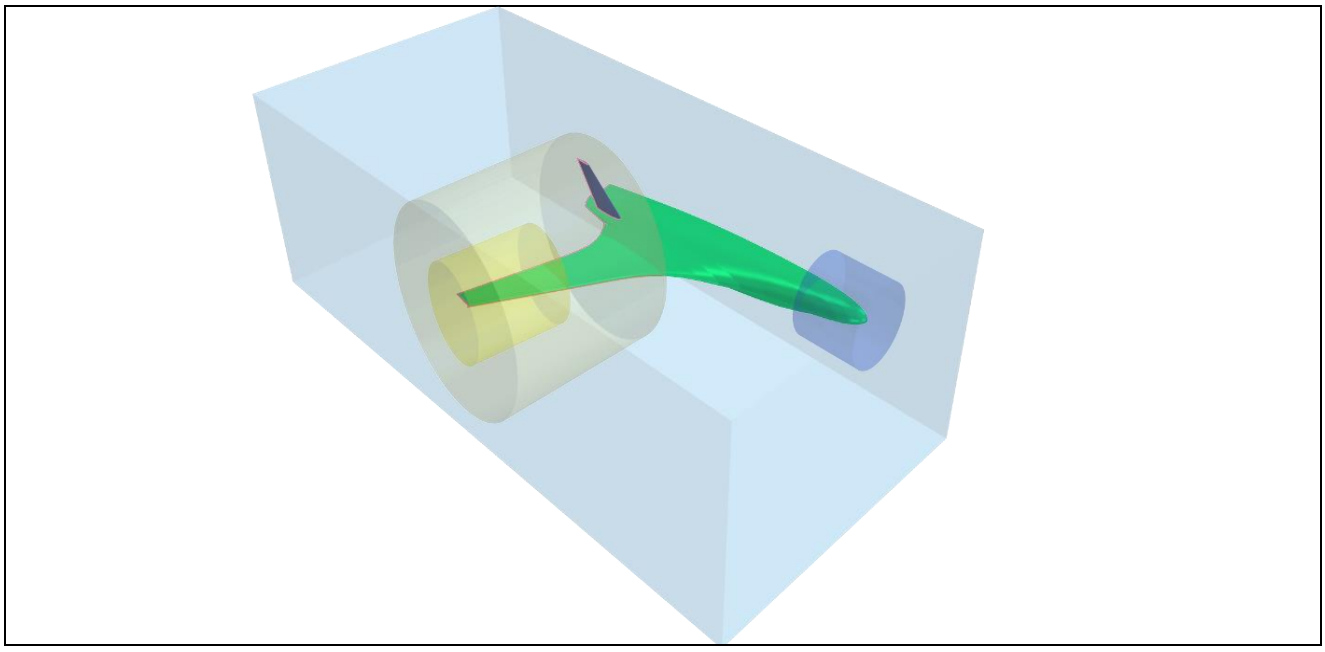

FIGURE 3 ALL MESH REFINEMENTS (MAIN WING, TRAILING EDGE OF THE BODY, WING TIP AND VERTICAL STABILIZER TIP) AND CUSTOM CONTROLS

A mesh independence study was done for an angle of attack 4.19^0 which is shown in the below table:

Base Size (m)	Number of Cells (Mio.)	C_L	C_D
0.85	11.10	0.19882	0.01192
0.77	13.92	0.19842	0.01189
0.60	19.56	0.19739	0.01183

TABLE 3 MESH INDEPENDENT ANALYSIS WITH LIFT COEFFICIENT TAKEN AS THE TEST PARAMETER

From the table above, we can observe that the variation in the lift coefficient and drag coefficient parameters are minimal for a large change in the number of cells (base size). Hence mesh independence can be concluded. As mesh independence has been achieved, we will be using the mesh with minimum cells (11.10 million) for our simulations to save time and memory usage.

4. Simulation Results and Discussion

4.1 Lift Coefficient

The simulated lift coefficients for all angle of attacks are shown below, along with the experimental data taken from. From the results we can observe that the experimental and simulation data are fairly close. The deviations in the values are presumed to occur due to the absence of droop and nacelles in the simulation model and the choice of the turbulence model.

AoA (^{O})	C_L simulation	C_L experiment	Abs. error	Rel. error (%)
4.19	0.1988	0.2331	-0.0343	-14.71
8.36	0.4153	0.4443	-0.0290	-6.51
12.53	0.5185	0.6380	-0.1195	-18.73

TABLE 4 COMPARISON OF LIFT COEFFICIENT FROM SIMULATED RESULTS AND EXPERIMENTAL DATA TAKEN FROM

4.2 Drag Coefficient

The simulated lift coefficients for all angle of attacks are shown below, along with the experimental data taken from. From the results we can observe that the experimental and simulation data are close and the deviations occur for similar reasons as the deviations in lift coefficient values, but a substantial gain in drag is observed at an AoA of 12.53^0. This can be explained by a lack of turbulence in the experiment but a high amount of turbulence in the CFD simulation. Furthermore, the k-ω SST model has a tendency to produce extremely high turbulences at stagnation regions.

AoA (^{O})	C_D simulation	C_D experiment	Abs. error	Rel. error (%)
4.19	0.0119	0.0147	-0.0028	-18.63
8.36	0.0239	0.0264	-0.0025	-9.54
12.53	0.0691	0.0468	+0.0223	+47.71

TABLE 5 COMPARISON OF DRAG COEFFICIENT FROM SIMULATED RESULTS AND EXPERIMENTAL DATA TAKEN FROM

4.3 Pressure Coefficient

The pressure coefficient distributions are shown in. The experimental data is taken from. The data is taken for 13.4% and 30.5% of the maximum half wingspan of the aircraft. The C_P plots for all 3 AoAs are shown below:

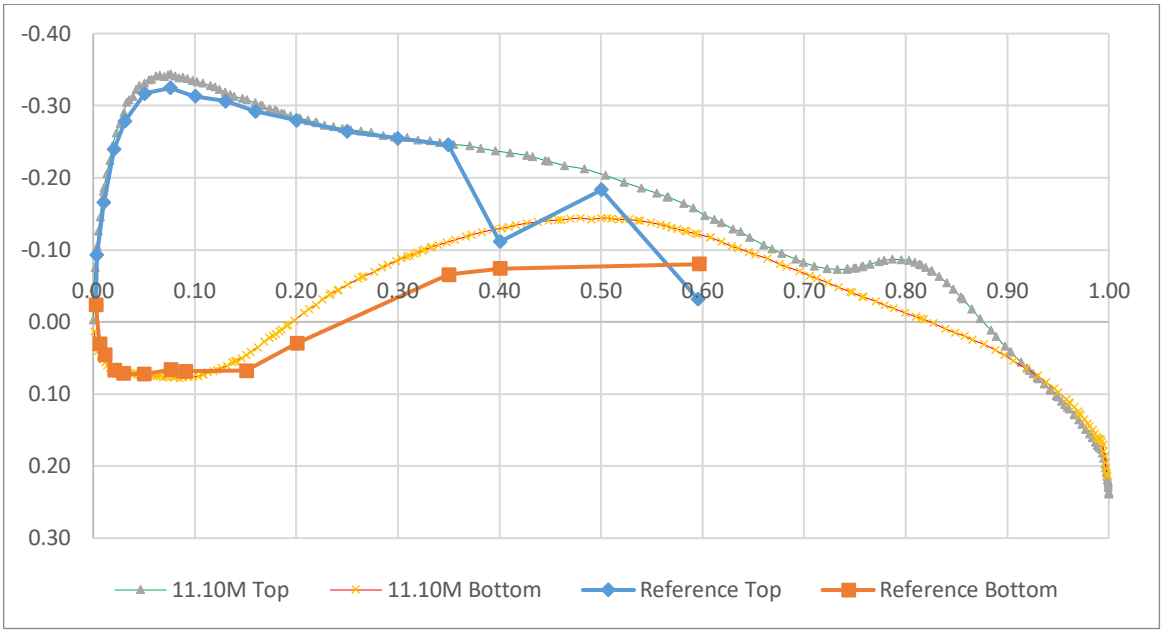

FIGURE 4 CP PLOT AT 13.4% HALF WINGSPAN FOR AOA 4.19 ^{O}

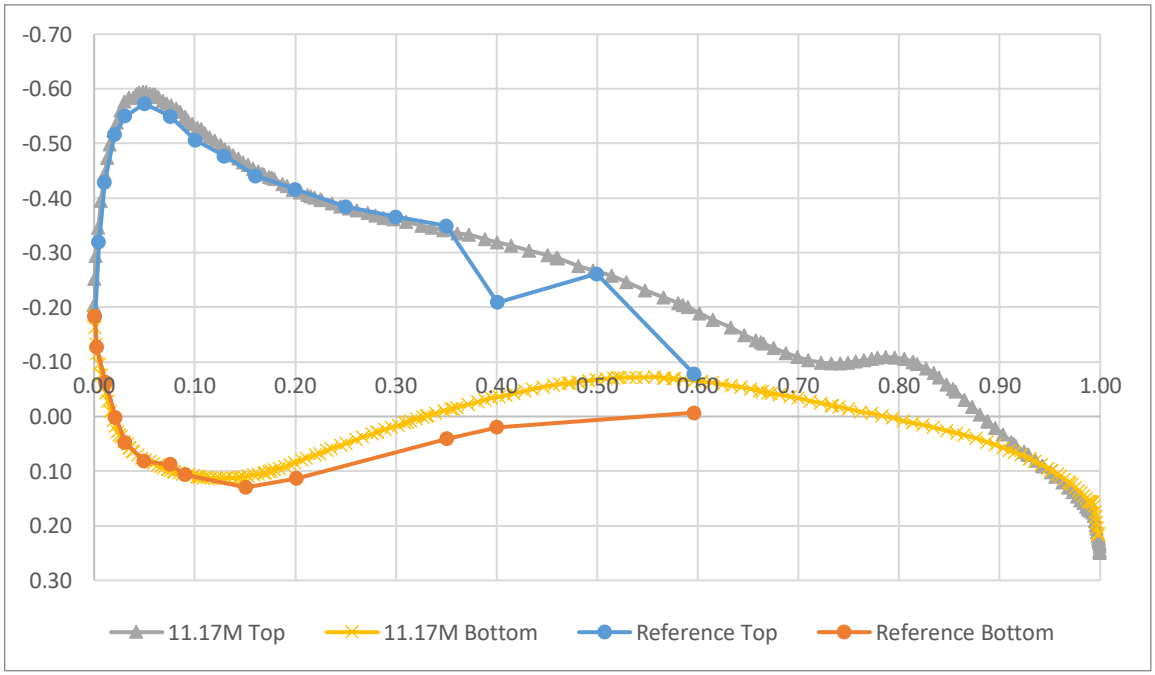

FIGURE 5 CP PLOT AT 13.4% HALF WINGSPAN FOR AOA 8.36 ^{O}

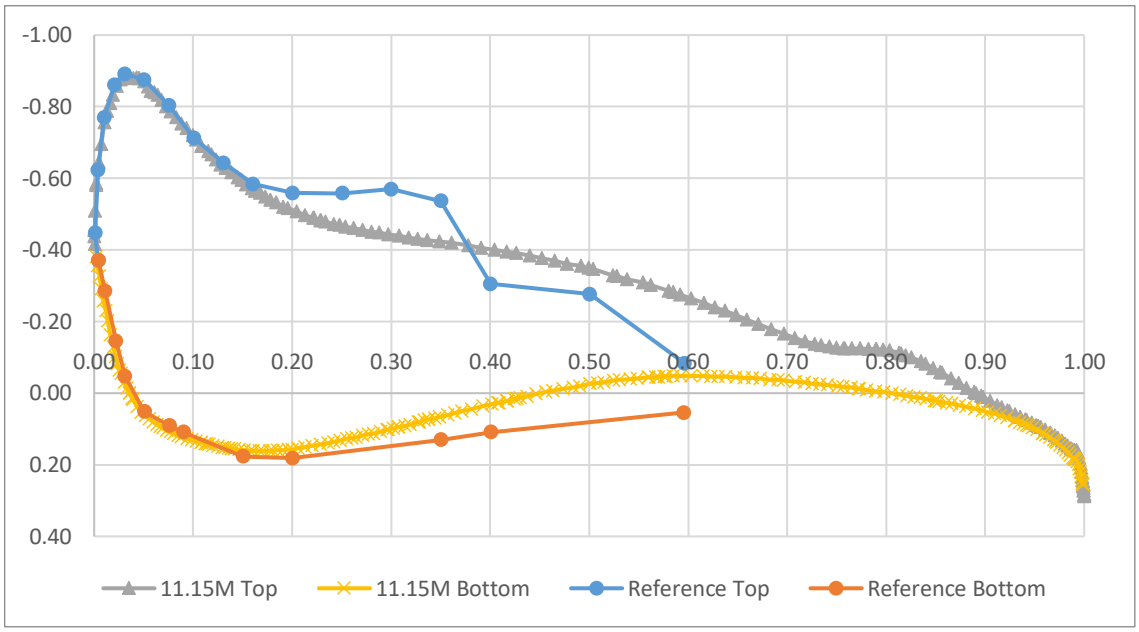

FIGURE 6 CP PLOT AT 13.4% HALF WINGSPAN FOR AOA 12.53 ^{O}

As seen in the graphs, the C_P plots at 13.4% half wingspan for all AoA are fairly similar until x/c = 0.12. From that point there is a small deviation in C_P up until the trailing edge in most cases. In the C_P plots at 13.4% for all AoA, it is observed that there is a drop in pressure coefficient on the top side of the wing just before x/c is 0.4. This can be explained due to the presence of a drooped edge in the experimental model. The drooped leading edge creates a higher acceleration on the upper side and an increase in pressure on the bottom side of the wing which results in an increase in C_P. Since there is no drooped edge present in the simulation model, there is no drop in C_P in this area.

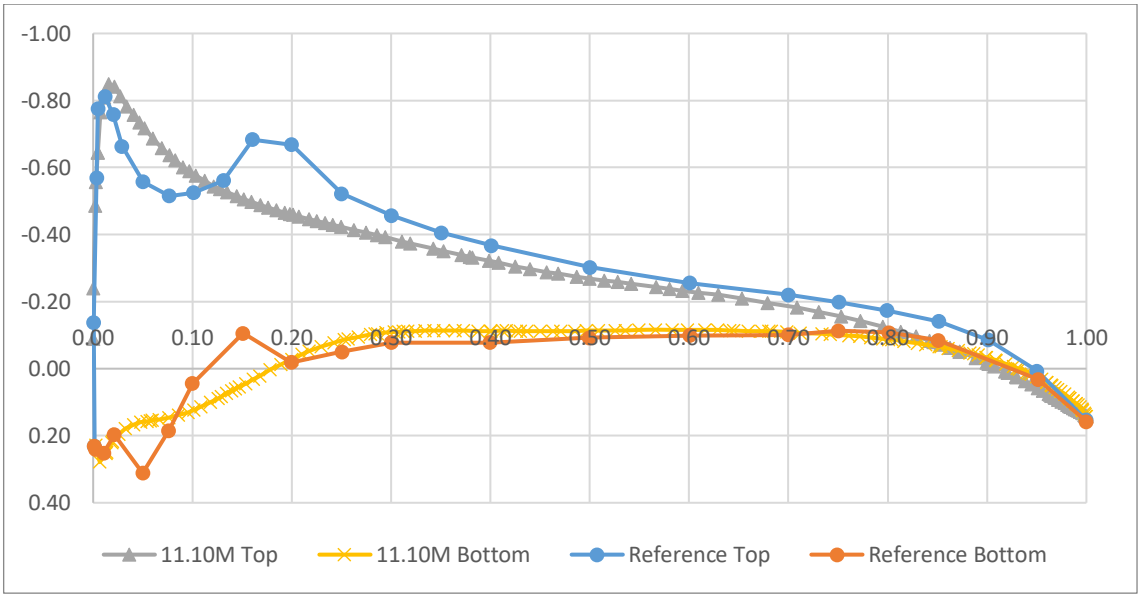

FIGURE 7 CP PLOT AT 30.5% HALF WINGSPAN FOR AOA 4.19 ^{O}

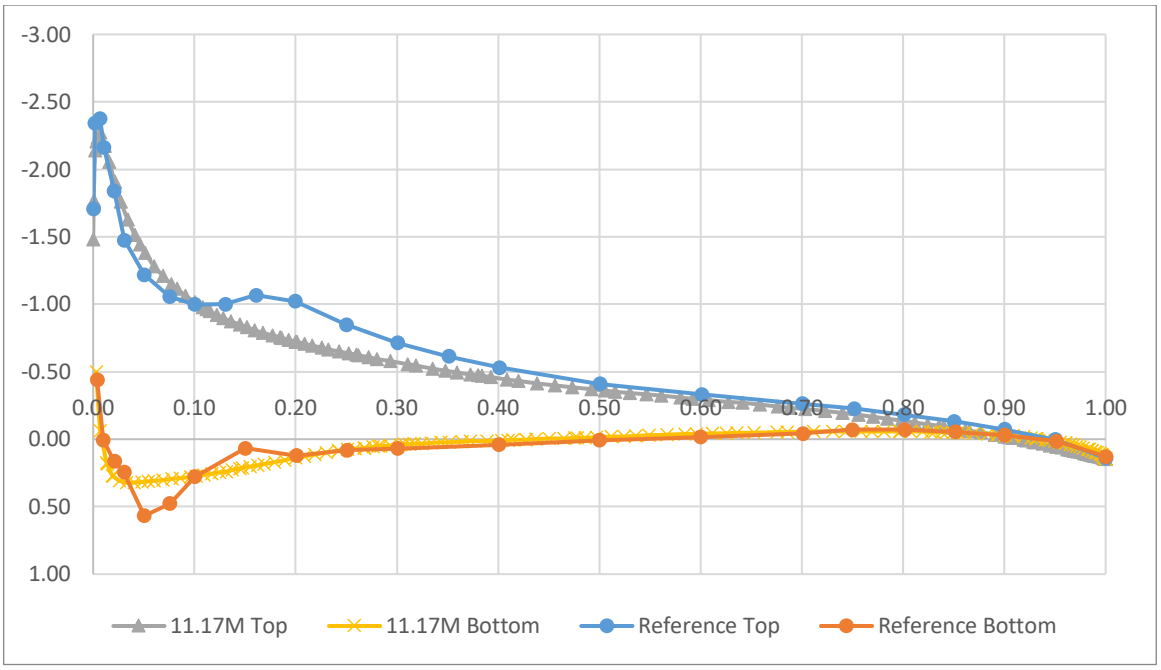

FIGURE 8 CP PLOT AT 30.5% HALF WINGSPAN FOR AOA 8.36 ^{O}

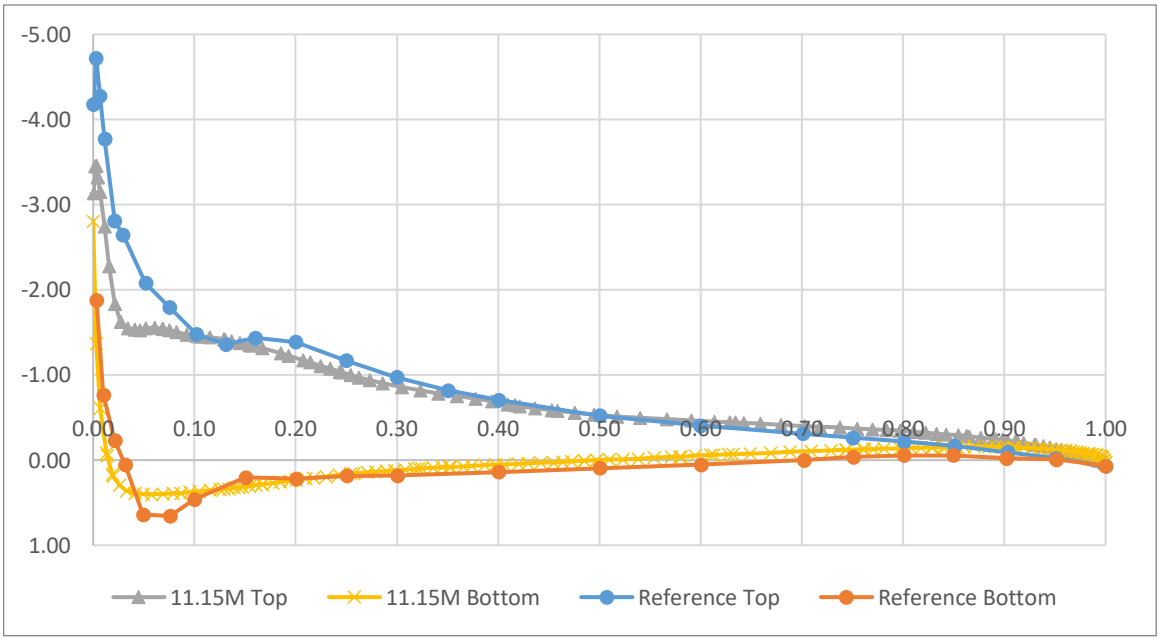

FIGURE 9 CP PLOT AT 30.5% HALF WINGSPAN FOR AOA 12.53 ^{O}

From the C_P plots at 30.5% half wingspan for all AoA it can be observed that the experimental and simulation values are very similar. The small deviations occurring at around x/c = 0.1 are again caused due to the use of a drooped edge in the experimental model. But the effect of the drooped edge is seen to be less significant in this area.

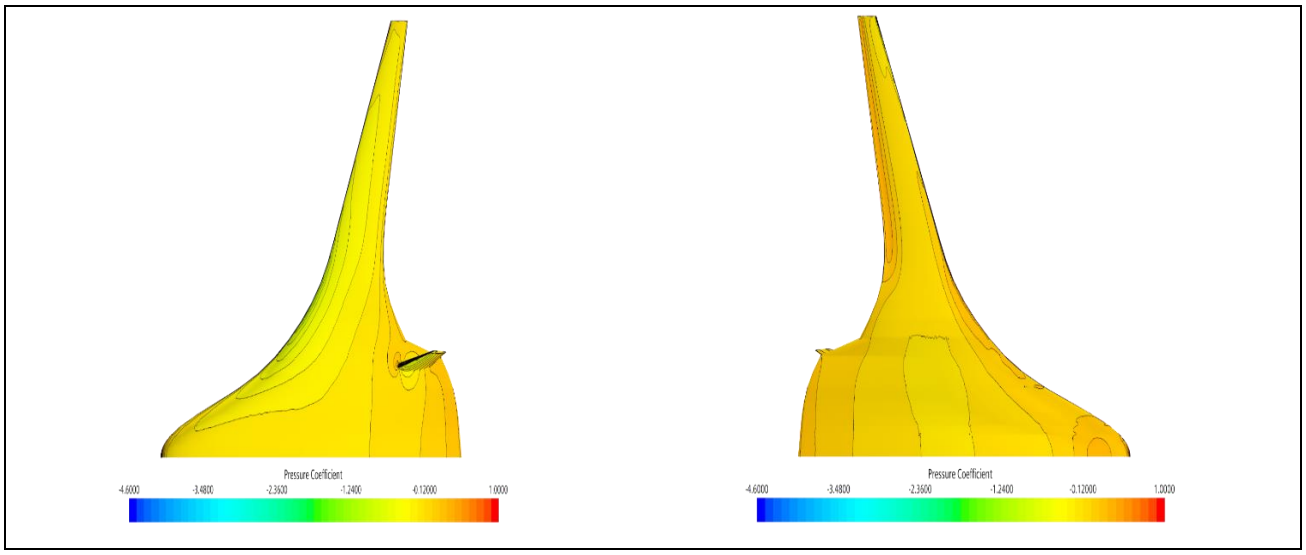

FIGURE 10 CP DISTRIBUTION OVER TOP (LEFT) & BOTTOM (RIGHT) OF THE MODEL FOR AOA 4.19 ^{O}

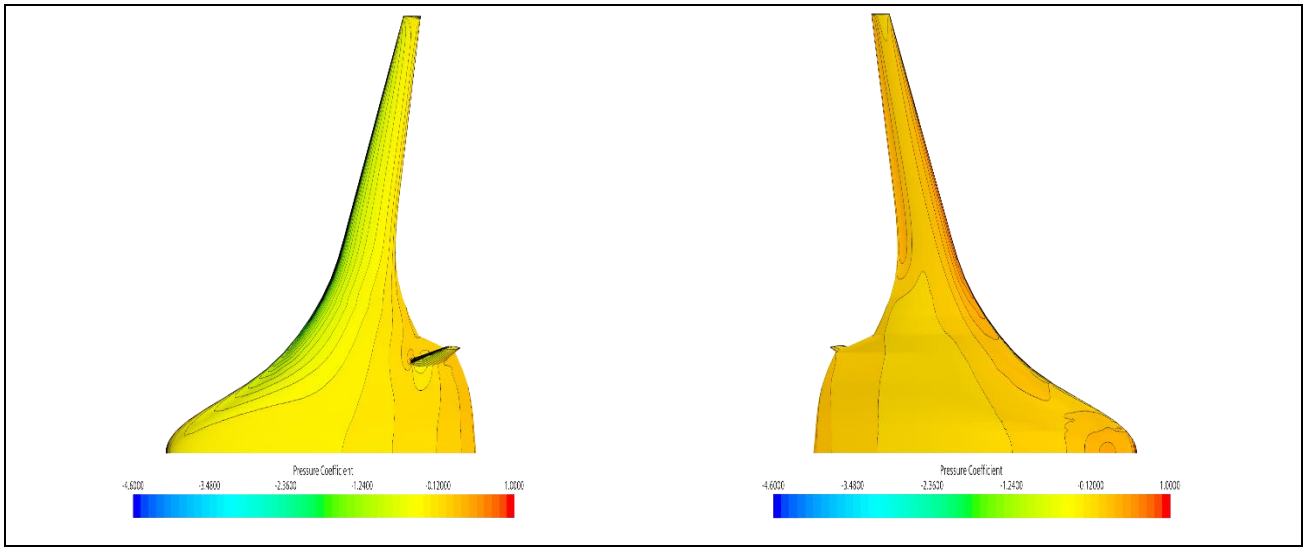

FIGURE 11 CP DISTRIBUTION OVER TOP (LEFT) & BOTTOM (RIGHT) OF THE MODEL FOR AOA 8.36 ^{O}

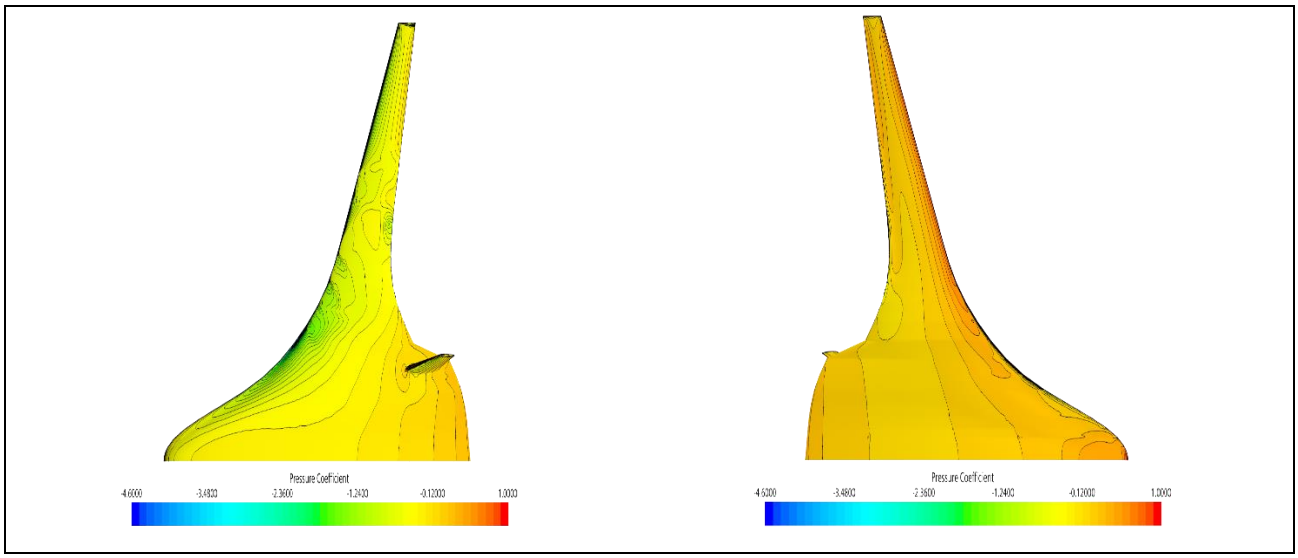

FIGURE 12 CP DISTRIBUTION OVER TOP (LEFT) & BOTTOM (RIGHT) OF THE MODEL FOR AOA 12.53^{O}

As seen in the C_P distribution images above, it can be noticed that the pressure coefficient is very high at the leading edge of the wing and gradually decreases as we reach the tail of the model which can be verified in the C_P distribution graphs at 13.4% and 30.5%. In the C_P distribution image for AoA 12.53^0, there are vortices forming on the top side which show turbulence, hence increasing the pressure coefficient and therefore generating more lift.

5. Conclusion

The simulation performed appears to display sufficiently accurate results. As there is a lack of certain configurations on the simulation model, a perfect comparison is not possible. But from an aerodynamic point of view the results are quite realistic and feasible. The deviations in values from the experimental data are concluded to be a result of the lack of drooped edges and nacelles. The experimental setup produces higher lift and drag coefficient compared to the simulation data due to the presence of these added configurations. A drawback of the usage of a k-ω SST turbulence model is the drastic increase in drag in areas of turbulence.

6. References

[1] Gatlin, G. M., Vicroy, D.D., Carter, M.B., "*Experimental Investigation of the Low-Speed Aerodynamic Characteristics of a 5.8-Percent Scale Hybrid Wing Body Configuration*", NASA Langley Research Center, June 2012

[2] Almosnino, D, "*A Low Subsonic Study of the NASA N2A Hybrid Wing-Body Using an Inviscid Euler-Adjoint Solver* ", Aerion Technologies Corporation / Desktop Aeronautics, Palo Alto, June 2016

APPENDIX

Flow field (Bullet shape)	
Radius	26 m
Length	39 m
Default Controls	
Base size	2.61 m
Target surface size	50 %
Minimum surface size	10 %
Surface Curvature	80 pts/circle
Surface Growth rate	1.15
Number of Prism Layers	20
Prism Layer near Wall Thickness	5.8E-6 m
Prism Layer Total Thickness	0.0246 m
Volume Growth Rate	1.05
Custom Controls	
Trailing Edge (Curve Control):	
Target Surface size	0.0025 m
Minimum Surface Size	0.00025 m
Wing and vert. Stabilizer (Curve Control):	
Target Surface size	0.001
Minimum Surface Size	0.00025 m
Main Body (Surface Control):	
Target Surface size	0.01 m
Minimum Surface Size	0.00025 m
Wake Refinement	7m/7.5 deg
Isotropic size	2 %
Wing Tips (Surface Control):	
Target Surface size	0.001 m
Minimum Surface Size	5E-4 m
Fuselage Wing Intersection (Volume Control):	
Prism Layer Total Thickness	0.019 m
Main Wing (Volume Control):	
Prism Layer Total Thickness	0.009 m
Nearfield (Volume Control):	
Isotropic size	2 %
Wake (Volume Control):	
Dimensions (y, z)	7.5 m x 5 m
Isotropic Size	10 %
Wing Tips (Volume Control):	
Isotropic Size	0.003 m